Developmental Biology 334 (2009) 46–58

Contents lists available at ScienceDirect

Developmental Biology

journal homepage: www.elsevier.com/developmentalbiology

D quadrant specification in the leech *Helobdella*: Actomyosin contractility controls the unequal cleavage of the CD blastomere

Deirdre C. Lyons *, David A. Weisblat

Department of Molecular and Cell Biology, 385 Life Sciences Addition, University of California, Berkeley, CA 94720-3200, USA

ARTICLE INFO

Article history:
Received for publication 28 April 2009
Revised 27 June 2009
Accepted 4 July 2009
Available online 14 July 2009

Keywords:
D quadrant specification
Lophotrochozoa
Actomyosin
Chirality
Spindle orientation
Spiral cleavage

ABSTRACT

The unequal division of the CD blastomere at second cleavage is critical in establishing the second embryonic axis in the leech *Helobdella*, as in other unequally cleaving spiralians. When CD divides, the larger D and smaller C blastomeres arise invariantly on the left and right sides of the embryo, respectively. Here we show that stereotyped cellular dynamics, including the formation of an intercellular blastocoel, culminate in a morphological left–right asymmetry in the 2-cell embryo, which precedes cytokinesis and predicts the chirality of the second cleavage. In contrast to the unequal first cleavage, the unequal second cleavage does not result from down-regulation of one centrosome, nor from an asymmetry within the spindle itself. Instead, the unequal cleavage of the CD cell entails a symmetric mitotic apparatus moving and anisotropically growing rightward in an actomyosin-dependent process. Our data reveal that mechanisms controlling the establishment of the D quadrant differ fundamentally even among the monophyletic clitellate annelids. Thus, while the homologous spiral cleavage pattern is highly conserved in this clade, it has diverged significantly at the level of cell biological mechanisms. This combination of operational conservation and mechanistic divergence begins to explain how the spiral cleavage program has remained so refractory to change while, paradoxically, accommodating numerous modifications throughout evolution.

Introduction

The distinctive mode of early development known as spiral cleavage is characteristic of disparate invertebrate taxa, including annelids, molluscs, polyclad flatworms and other, less-speciose phyla all belonging to the super-phylum Lophotrochozoa (Dunn et al., 2008; Giribet, 2008; Halanych et al., 1995). Spiralian development therefore offers unique opportunities for examining how the evolution of divergent body plans is achieved by developmental innovations within a conserved embryological framework.

One example of evolutionary flexibility within the spiral cleavage program is D quadrant specification (Freeman and Lundelius, 1992; Henry and Martindale, 1999). In spiral cleavage, the first two cell divisions are roughly meridional with respect to the animal–vegetal axis, establishing four embryonic quadrants (A–D). By convention, D is defined as the dorsal quadrant, which produces bilaterally symmetric trunk mesoderm and ectoderm (Dorresteijn, 2005; Lambert, 2008; Shimizu and Nakamoto, 2001; van den Biggelaar and Guerrier, 1983; Verdonk and van den Biggelaar, 1983). Thus, selecting one quadrant to be the D quadrant is fundamental to forming the second embryonic axis.

Although D quadrant specification is homologous among spiralians, significant variations in this process have evolved (Freeman and Lundelius, 1992). In equally cleaving species, the first two rounds of mitosis give rise to four blastomeres of equal developmental potential, and typically of equal size; only later is one of the quadrants selected stochastically to adopt the D fate (Arnolds et al., 1983; Martindale et al., 1985; van den Biggelaar and Guerrier, 1979). In unequally cleaving species, the D quadrant is established at the 4-cell stage by two unequal cleavages that segregate developmental determinants to one quadrant; typically the D blastomere is larger than the A, B and C blastomeres (Astrow et al., 1987; Clement, 1952; Dorresteijn et al., 1987). Equal cleavage is thought to be the ancestral state for spiralians, and unequal cleavers occur on various branches of the phylogenetic tree relating spiralian taxa. This suggests that changes from equal to unequal division have occurred multiple times and thus that D quadrant specification via unequal division is not homologous across spiralians (Freeman and Lundelius, 1992; Henry, 1986; Henry et al., 2006).

Evidence regarding intrinsic and extrinsic factors controlling unequal cell divisions in spiralian embryos have come from diverse annelids and molluscs (Dorresteijn, 2005; Goulding, 2003; Hejnol and Pfannenstiel, 1998; Inoue and Dan, 1987; Lambert and Nagy, 2001; Luetjens and Dorresteijn, 1998a; Mescheryakov, 1976; Schneider and Bowerman, 2007; Shibazaki et al., 2004; Shimizu et al., 1998; Zhang and Weisblat, 2005). To understand how a process such as D

* Corresponding author.
E-mail addresses: dclyons@berkeley.edu (D.C. Lyons), weisblat@berkeley.edu (D.A. Weisblat).

0012-1606/$ – see front matter © 2009 Elsevier Inc. All rights reserved.
doi:10.1016/j.ydbio.2009.07.007

quadrant specification evolved, we must compare the underlying cell biological and molecular mechanisms in various species whose phylogenetic relationships are also understood. Clitellate annelids, a well-accepted monophyletic group comprising leeches (Hirudinea) and oligochaetes (Erseus and Kallersjo, 2004; Siddall and Borda, 2003; Siddall and Burreson, 1998), provide a number of experimentally tractable species for making such comparisons (Dohle, 1999; Shankland and Savage, 1997; Shimizu and Nakamoto, 2001; Weisblat, 2007). The monophyly of the clitellates allows us to make evolutionary comparisons between homologous cleavage patterns.

Detailed knowledge of clitellate embryogenesis comes primarily from studies of glossiphoniid leeches of the genera *Helobdella* and *Theromyzon* (Fernández and Olea, 1982; Weisblat and Huang, 2001) and tubificid oligochaetes of the genus *Tubifex* (Shimizu, 1982a). Essentially all clitellate embryos exhibit the following features, which are therefore considered homologous within this group. Prior to first cleavage, cytoplasmic rearrangements form domains of yolk-deficient cytoplasm, called teloplasm, that are rich in organelles and polyadenylated mRNA (Fernández et al., 1990). Teloplasm is segregated to the D quadrant and contains factors necessary for the formation of stem cells (teloblasts) that make segmental ectoderm and mesoderm (Astrow et al., 1987; Ishii and Shimizu, 1997; Nelson and Weisblat, 1991, 1992). The first cleavage results in a smaller AB cell and a larger CD cell, which inherits teloplasm. At second cleavage the CD cell divides to form a smaller C cell and a larger D cell, which inherits teloplasm. Thus, the unequal first and second cleavages establish the axes of the adult by segregating teloplasm exclusively to the D quadrant at the 4-cell stage (Weisblat et al., 1999).

Although the clitellate cleavage pattern is highly conserved, it has been shown that the mechanisms controlling teloplasm formation (Astrow et al., 1989; Shimizu, 1982b) and the unequal first cleavage (Ishii and Shimizu, 1997; Ren and Weisblat, 2006) are divergent between *Helobdella* and *Tubifex*. Specifically, teloplasm formation is a microtubule-dependent process in *Helobdella* and a microfilament-dependent process in *Tubifex* (Astrow et al., 1989; Shimizu, 1982a,b). Also, in *Tubifex*, the unequal first cleavage involves a non-duplicating, maternally-derived centrosome so that the mitotic apparatus is monoastral and highly asymmetric throughout first cleavage (Ishii and Shimizu, 1995, 1997; Shimizu, 1982a,b), whereas in *Helobdella*, the centrosome is paternally-derived and duplicates early in the first cell cycle. The resultant biastral mitotic apparatus (MA) in *Helobdella* is symmetric through early metaphase; then, one centrosome is down-regulated, followed by the partial collapse of the associated aster, which renders the MA asymmetric and leads to the unequal first cleavage (Ren and Weisblat, 2006). These studies demonstrated that despite the fact that teloplasm formation and unequal first cleavage are homologous events in clitellates, the cell biological mechanisms controlling them are different. Comparing the mechanisms controlling D quadrant specification in *Helobdella* versus *Tubifex* therefore gives us clues about the evolutionary constraints and permissions of the spiral cleavage program.

The work presented here extends these comparisons by addressing the mechanisms underlying the inequality and chirality of the CD cleavage in *Helobdella* (Fig. 1). We show that the unequal cleavage of the CD cell entails an intimate connection between the mitotic apparatus and the cortex at the interface between the AB and CD cells. The CD spindle is symmetric and biastral and attaches via both asters to the cortex surrounding an intercellular blastocoel that forms during the 2-cell stage. The CD MA initially resides equidistant from the edges of the CD cell and subsequently becomes displaced toward the right side of the cell beginning in metaphase, inducing an eccentrically located cytokinetic furrow. Pharmacological perturbation of the microtubule and actomyosin cytoskeletons revealed that: 1) the intimate connection between the spindle poles and the basolateral cortex is necessary for proper spindle orientation and 2) the rightward movement of the mitotic apparatus is controlled by actomyosin contractility. We discuss the evolutionary implications of these findings in the context of D quadrant specification in relation to *Tubifex* and other spiralians.

Methods and materials

Animal culture and embryonic timing

Embryos were obtained from a permanent laboratory culture of *Helobdella* sp. (Austin), originating from Austin, Texas (Bely and Weisblat, 2006). *Helobdella* zygotes are deposited one by one, so each clutch (20–100 zygotes) is slightly asynchronous. For precise timing, developmental events are designated as occurring at a particular time after zygote deposition (AZD) (Weisblat and Huang, 2001; Yazdani and Terman, 2006) at 23 °C. We grouped embryos that had begun first cleavage (as judged by the first deformation of the plasma membrane) within a 5-minute window (usually 3–10 embryos) and defined this group as 265 ± 2.5 min AZD. Embryos were cultured at 23 °C in Htr medium (Blair and Weisblat, 1984).

Immunohistochemistry

Fixation and immunostaining were carried out as for the zygote (Ren and Weisblat, 2006). Mouse monoclonal antibody against beta-tubulin (Sigma, T-0198 clone number D66) was used at 1:1000; rabbit polyclonal antibody against sea urchin tubulin was a gift of the Cande lab at U.C. Berkeley and was used at 1:25; rabbit polyclonal antibody against gamma-tubulin (Sigma, T-3559) was used at 1:2000; rabbit polyclonal antibody against actin (Sigma, A2066) was used at 1:50; mouse monoclonal antibody against histone H1 (Chemicon, MAB052) was used at 1:2000; rabbit polyclonal antibody against myosin light chain (phospho S20; AbCam, ab2480) was used at 1:500. Alexa fluor-labeled fluorescent secondary antibodies (Molecular Probes) were used at 1:500; Cy3- and Cy5-labeled antibodies (Jackson Immunosciences) were used at 1:800; Cy2-labeled antibodies (Jackson Labs) were used at 1:50. Following immunohistochemistry, embryos were dehydrated through an ethanol series and cleared in 3:2 benzyl benzoate:benzyl alcohol (BBBA) for confocal microscopy.

Drug treatments

Primary stocks of nocodazole (20 μM, Sigma, M1404), cytochalasin D (25 mM, Sigma, C8273), and blebbistatin (100 mM, Toronto Research Chemicals, B592500) were made in DMSO and stored at −20 °C. Primary stock of ML-7 (300 μM, Calbiochem, 475880) was made in DMSO and stored at 4 °C. Working stocks were prepared immediately prior to use by dilution with Htr; control embryos were incubated in matching dilutions of DMSO (0.2–0.05%). For all drug treatments, each group of embryos undergoing their first cleavage within a 5-minute window (see above) was split and immediately immersed in drug or control solutions and incubated at room temperature throughout the 2-cell stage for live observations or subsequent fixation and immunohistochemistry. Three or more experiments were performed for each drug treatment.

Microscopy, imaging software and image analysis

Live embryos were viewed with a dissecting microscope under fiber optic illumination. Images were captured with a digital camera (Nikon cool pix) mounted on the dissecting microscope. Immunostained and BBBA-cleared embryos were examined by laser scanning

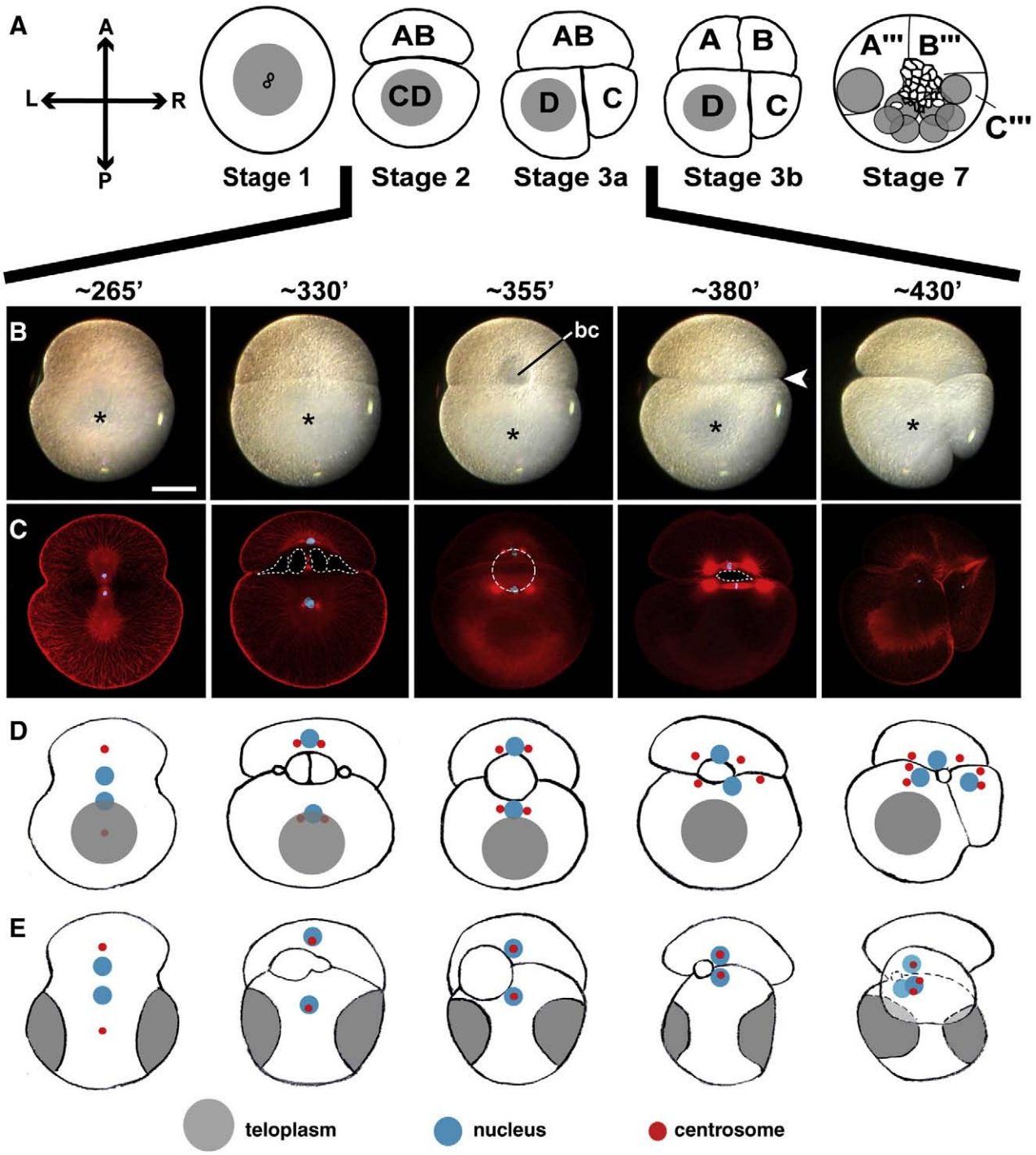

Fig. 1. Unequal second cleavage during D quadrant specification in *Helobdella*. (A–D) Stages of early leech development. Animal pole views with AB cell at the top, except as noted; the prospective adult axes are indicated at left (A, anterior; P, posterior; L, left; R, right). (A) Yolk-deficient cytoplasm (teloplasm; gray) forms at animal and vegetal poles in the zygote after polar bodies (small circles) have formed (stage 1). At the end of cleavage (stage 7), the embryo comprises 5 pairs of D-derived segmentation stem cells (teloblasts; gray circles). (B) Live embryos viewed at selected time points during stages 2 and 3a; developmental times given in minutes after zygote deposition (AZD; prior to 350′ AZD the animal and vegetal poles cannot be distinguished so these may be either animal or vegetal views). Teloplasm (asterisks) is visible throughout; a blastocoel (bc) becomes visible in live embryos by 355′. The embryos are initially bilaterally symmetric along the AB–CD axis, but by 380′, AB and CD are more tightly apposed on the right side of the embryo than on the left (arrowhead), predicting the unequal CD cleavage. (C) Confocal images of embryos fixed at the time points shown in (B) and stained with antibodies to sea urchin tubulin (red) and mouse histone 1 (blue). The blastocoel (dotted contours) becomes visible as interconnected pockets by 330′ AZD; at 355′ AZD, the blastocoel (dotted circle) lies outside the plane of the section shown, as illustrated in (E). (D) Schematic illustrations showing the spatial relationship of blastocoel, spindle poles and teloplasm; microtubules are omitted for simplicity. (E) Equatorial views of the stage shown in (D) with AB at the top and animal pole to the left. Scale bar, 100 μm.

confocal microscopy (Zeiss 510 Axioplan META with Zeiss LSM software or Leica DM RE with Leica TCS software). Image analysis and measurements were made with LSM and ImageJ software. Multiple confocal slices were manually montaged using Adobe Photoshop or converted into maximum intensity projections using ImageJ (Jackson et al., 2001).

Results

D quadrant specification in Helobdella

Based on the work from *H. triserialis* (Bissen and Weisblat, 1989) we assumed that there is no G1 phase in the early cell cycles of the closely related *H.* sp. (Austin) used in this study. The plane of the unequal first cleavage (265′ AZD) is separate from, but parallel to, the animal–vegetal axis (A/V). This results in a larger CD cell, which inherits both pools of teloplasm, and a smaller AB cell (Fig. 1). The AB–CD axis is roughly parallel to the anterior–posterior axis (Weisblat et al., 1999). The second cleavage planes are parallel to the A/V axis, and perpendicular to the plane of the first division, but second cleavage is asynchronous, with CD initiating cytokinesis before AB (400′ AZD and 430′ AZD, respectively). Cell CD also divides unequally, yielding a smaller C cell and a larger D cell, which inherits both pools of teloplasm.

Cellular dynamics and the appearance of left–right asymmetry during the 2-cell stage

To investigate the cellular mechanisms regulating the unequal CD division, we made time lapse movies of embryonic development from the zygote to the 4-cell stage (Fig. 1B). These movies revealed systematic changes in shape and extent of apposition of the AB and CD blastomeres (Figs. 1B, 2). Following cytokinesis of the zygote (265′–285′ AZD; Fig. 1), the embryo underwent a transient period during which the AB and CD blastomeres flattened against each other and the area of direct contact between the two cells increased (310′–350′ AZD; Figs. 1, 2B). At the peak of this process (330′–345′ AZD; Figs. 1, 2B), the area of contact between AB and CD was maximal. During a subsequent phase (345′–370′ AZD; Figs. 1, 2B), the cells became more rounded and the area of contact between them was reduced (Figs. 1, 2B).

The AB and CD cells remained bilaterally symmetric throughout the periods of cytokinesis and flattening (Figs. 1, 2). The first signs of left–right (L–R) asymmetry were seen at 365′–370′ AZD (Figs. 1, 2), when the AB and CD cells started to become more apposed on the right side of the embryo (Fig. 1B arrowhead). Consequently, the zone of apposition became progressively displaced towards the right side of the embryo (Fig. 2B).

Time-lapse observations of live embryos were complemented with confocal microscopy of embryos fixed at selected time points relative to first cleavage, then doubly labeled with cross-reactive antibodies for histone H1 and tubulin to mark chromatin and microtubules, respectively (Figs. 1C, 3A). This analysis revealed that, in contrast to first cleavage, the MAs of cells AB and CD lie close to the cortex where AB and CD are apposed. This aspect is described in more detail below. The CD cell was in interphase from 265′ AZD to approximately 350′ AZD (Figs. 1, 3). CD mitosis (350′–395′ AZD) comprised 20′ prometaphase, 20′ metaphase, and 5′ anaphase. Telophase began coincident with the initiation of cytokinesis (Fig. 3A). The cytokinetic furrow was first evident in confocal images beginning at ~400′ AZD, deep in the cell, next to the spindle midpoint (Fig. 3A). In live embryos, the furrow was first visible at approximately 405′ AZD (Fig. 6B) at the anterior of the cell. The furrow then extended towards the posterior side of the

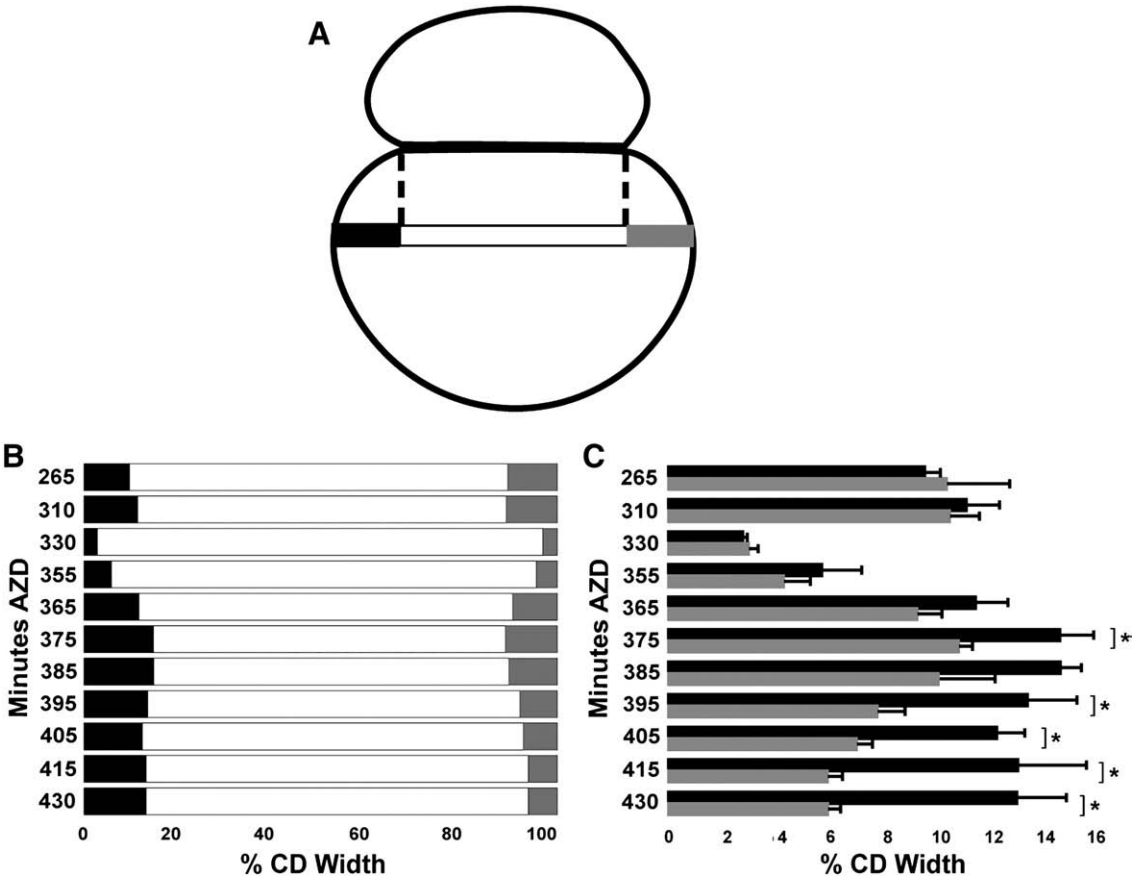

Fig. 2. Dynamics of blastomere contact during the 2-cell stage. (A) Schematic depicting the measurements taken from images of live embryos (see Fig. 1B) at time points shown in (B) and (C). The maximum width of CD perpendicular to the AB–CD axis (tri-colored bar) is defined as 100%. (B) Graphical representation of the changes in width and relative position of the interface, averaged from 3–5 embryos per time point; error bars for the overhangs are shown in (C). (C) Systematic loss of bilateral symmetry midway through the 2-cell stage is revealed by comparing the average and standard deviation of the left (black bars) and right (gray bars) overhangs. The left and right sides of the embryo differ significantly (*) starting at 375′ ($p \leq 0.01$, Student's *t*-test).

CD cell, which deformed at ~415′ AZD. AB cell mitosis (375–425′ AZD) comprised 20′ prometaphase, 25′ metaphase, and 5′ anaphase, and telophase began coincident with the initiation of cytokinesis at 425′ AZD.

By comparing time lapse and confocal data, we concluded that the first visible L–R asymmetry in the embryo coincided with the prophase–metaphase transition of the CD cell (365–375′ AZD; Figs. 1B, 2C, 3A, E).

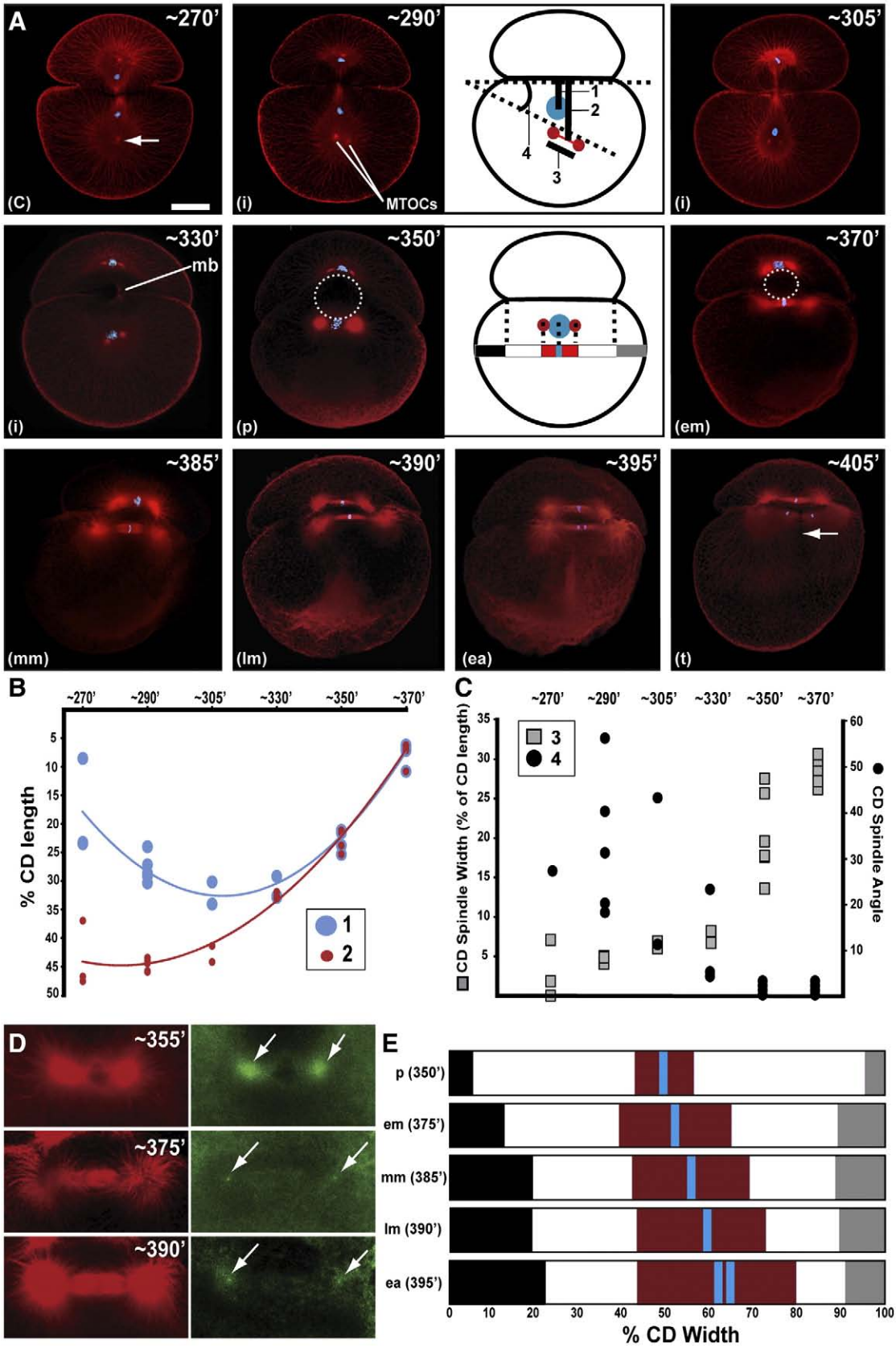

A transient blastocoel forms during the 2-cell stage

The confocal microscopic examination of immunostained embryos also revealed details of the formation of an intercellular cleavage cavity or blastocoel that has been described in the early embryos of other freshwater spiralians (Raven, 1966; Verdonk and van den Biggelaar, 1983). We noticed that beginning at approximately 310′ AZD the membranes at the center of the interface between the AB and CD cells separated, creating multiple intercellular pockets (Figs. 1C–E, 3A). From multiple series of fixed, immunostained embryos we inferred a gradual process in which the pockets fused and inflated between 310′ AZD and 355′ AZD to form a single large blastocoel cavity, which became visible in live embryos starting around 340′ AZD (Fig. 1B). At its largest, the blastocoel resided at the center of the embryo in the left–right axis and was situated towards the animal pole (Figs. 1D, E). As the CD cell proceeded through mitosis, the blastocoel shrank and became displaced to the right side of the embryo, eventually disappearing.

The presence of the blastocoel meant that three topologically distinct domains of cell membranes and cortical cytoplasm could be distinguished in the 2-cell embryo: an apical domain consisting of the outer surfaces of AB and CD, and two basolateral domains, one consisting of the walls of the blastocoel itself and the other consisting of the zone of direct apposition between AB and CD. The two basolateral domains will be referred to collectively as the AB/CD interface.

The CD mitotic apparatus comes to lie in contact with the interface cortex and remains symmetric throughout mitosis

First mitosis in *Helobdella* involves a reduced contribution from anaphase A relative to anaphase B (Ren and Weisblat, 2006). Thus, at the end of the first cleavage, the CD centrosome lies far from the nucleus (Figs. 1C, 3A); even after the centrosomes had begun to separate in preparation for CD mitosis, they were far posterior to the CD nucleus and then moved anteriorly to capture the nucleus (Fig. 3A, B). While the movements of the centrosomes could not be observed in real time due to the light scattering by the yolky cytoplasm, we inferred some details of this process by measuring the spindle-interface angle and spindle width (the distance between the centrosomes) and the distances of the nucleus and spindle midpoint from the AB/CD interface in multiple embryos at 6 different time points (Figs. 3A–C). As expected, we found that the distance from the spindle midpoint to the interface decreased continuously (Fig. 3B) and the spindle width increased continuously (Fig. 3C) as the pair of centrosomes approached the nucleus. In contrast, the angle of the centrosome axis with respect to the interface varied erratically both within and between time points prior to 350′ AZD. One interpretation of this result is that, prior to this time point, the centrosomes exhibited a stepping or rocking motion in approaching the interface, in response to forces acting on both centrosomes, consistent with direct observations in other systems (Cowan and Hyman, 2004). If only one centrosome were under force and the other were being pulled passively, we would have expected the centrosome axis to be more uniformly perpendicular to the interface. Finally, we observed that the nucleus moved away from the interface prior to being captured by the centrosomes; this suggests that the nucleus was being pulled toward the centrosomes.

To determine whether the unequal second cleavage involves centrosomal down-regulation and an asymmetric MA as does the unequal first cleavage (Ren and Weisblat, 2006), we immunostained embryos for beta and gamma-tubulin (Fig. 3D) or histone and tubulin (Fig. 3A) at selected time points during CD mitosis (Fig. 3D). The following description reflects observations made on at least 3 embryos per time point for gamma-tubulin staining and at least 20 embryos per time point for tubulin staining.

At CD prophase (~350′ AZD) the MA spindle poles were closely apposed to the vegetal portion of the blastocoel wall (Fig. 3A). The chromatin lay midway between the spindle poles, each of which was associated with a centrosome as judged by gamma-tubulin immunoreactivity, and the astral arrays were of equal size as judged by eye (Fig. 3D). During metaphase, as the blastocoel shrank, the asters remained attached to the cortex, which became part of the zone of direct apposition between the cells (365′–390′ AZD; Fig. 3A). As mitosis proceeded, both spindle poles maintained a (gamma-tubulin-positive) centrosome (Fig. 3D) and the astral microtubule arrays of both poles remained similar in size (Figs. 3A, D). Within the asters, however, the microtubules shortened on the side of the spindle facing the basolateral domain (Figs. 1C, 3A). Tubulin staining failed to reveal any L–R asymmetry of microtubules that might correlate with the inequality of CD cleavage (Luetjens and Dorresteijn, 1998a).

Unequal CD cleavage entails the rightward displacement of a symmetric MA

Since the MA remains symmetric throughout mitosis (Figs. 3A, D), how does the unequal cleavage of cell CD come about? From observations of live embryos and our confocal microscopic analysis of the timed series of fixed embryos, we inferred that the eccentric placement of the CD cytokinetic furrow resulted from 2 factors: 1) during early metaphase the spindle moved towards the right side of the cell relative to the interface and 2) during later metaphase and anaphase the spindle elongated towards the right side of the embryo (Fig. 3E). There was no statistically significant difference in the chromosome-to-spindle distances for the C and D spindle poles ($n=6$), however the distance between the DNA and the center of the D spindle pole was always slightly larger.

The spindle remained closely apposed to the interface (~375′ AZD) and equidistant between the left and right sides of the embryo until early metaphase (Figs. 3A, E), which correlated with the symmetric apposition of the two blastomeres at this time (Fig. 2). During early metaphase the spindle was also positioned in the center of the AB/CD

Fig. 3. Spindle dynamics leading to the unequal CD cleavage, inferred from (A) animal pole view confocal images of representative embryos fixed at indicated time points (min AZD) then immunostained for tubulin (red) and histone (blue). [Prior to 350′ the animal and vegetal poles cannot be distinguished, so embryos prior to this time may be animal or vegetal views.] When the first cleavage furrow has initiated (270′ AZD) the CD nucleus lies roughly midway between the future AB/CD interface and spindle pole inherited by the presumptive CD cell (arrow). By 290′ AZD, the spindle pole has given rise to two microtubule organizing centers (MTOCs). The MTOCs move anteriorly (305′ AZD) and contact the CD nucleus (330′ AZD); in this image the midbody (mb) is visible, spanning the blastocoel. The centrosome/nucleus complex approaches the interface, contacting first the vegetal portion of the blastocoel wall (dotted line, 350′ AZD) in prophase and then the zone of direct AB–CD apposition within the basolateral domain (370′). The MA remains symmetric and in contact with the interface but shifts rightward during metaphase and anaphase (370′–395′ AZD). By 405′ AZD, a microtubule deficient slit (arrow) is seen perpendicular to the spindle. This coincides with the position of the cytokinetic furrow (not yet visible in this focal plane). (c) = cytokinesis; (p) = prophase; (i) = interphase; (em) = early metaphase; (mm) = mid metaphase; (lm) = late metaphase; (ea) = early anaphase; (t) = telophase. (B) Distances of the nucleus and spindle midpoint from the AB/CD interface [measurements 1 and 2 in schematic at 290′ AZD in (A)]. (C) Plot of spindle-interface angle and spindle width during the 2-cell stage [measurements 3 and 4 in schematic at 290′ AZD in (A)]. (D) The CD MA remains symmetric both in terms of microtubule astral arrays (beta-tubulin, red) and centrosome persistence (gamma-tubulin, green; arrows). (E) Size and position of the MA relative to the AB/CD interface and the overall CD width during CD mitosis [see schematic for embryo at 350′ AZD in (A)]. In prophase (p) and early metaphase (em) the chromatin (blue), spindle (red) and AB/CD interface (white) are centered with respect to the left and right CD overhangs (black and gray, respectively). But in mid and late metaphase and early anaphase (mm, lm and ea, respectively), the spindle elongates by growing selectively to the right side, coincident with the rightward shift of the AB/CD interface. Measurements are averages from 3–5 embryos from each time point. Scale bar, 100 μm.

interface (Figs. 3A, E). During mid metaphase the symmetric CD MA began to shift towards the right side of the cell (Fig. 3E) as AB and CD were becoming more tightly apposed on the right side of the embryo, which had the effect of shifting the interface to the right side of the embryo (Fig. 2B). In addition, the spindle elongated anisotropically during anaphase, growing preferentially towards the right side of the embryo (Fig. 3E). Collectively, these events displaced the MA towards the right side of the CD cell. Since the cytokinetic furrow is induced by the MA (Glotzer, 2004; Rappaport, 1996), it, too, formed on the right side of the CD cell.

To test the possibility that the unequal second cleavage relies on communication between the mitotic apparatus and the cortex of the AB/CD interface, we examined the orientation and position of the MA (Fig. 4), as well as the inequality of the CD division (Figs. 5, 6), in

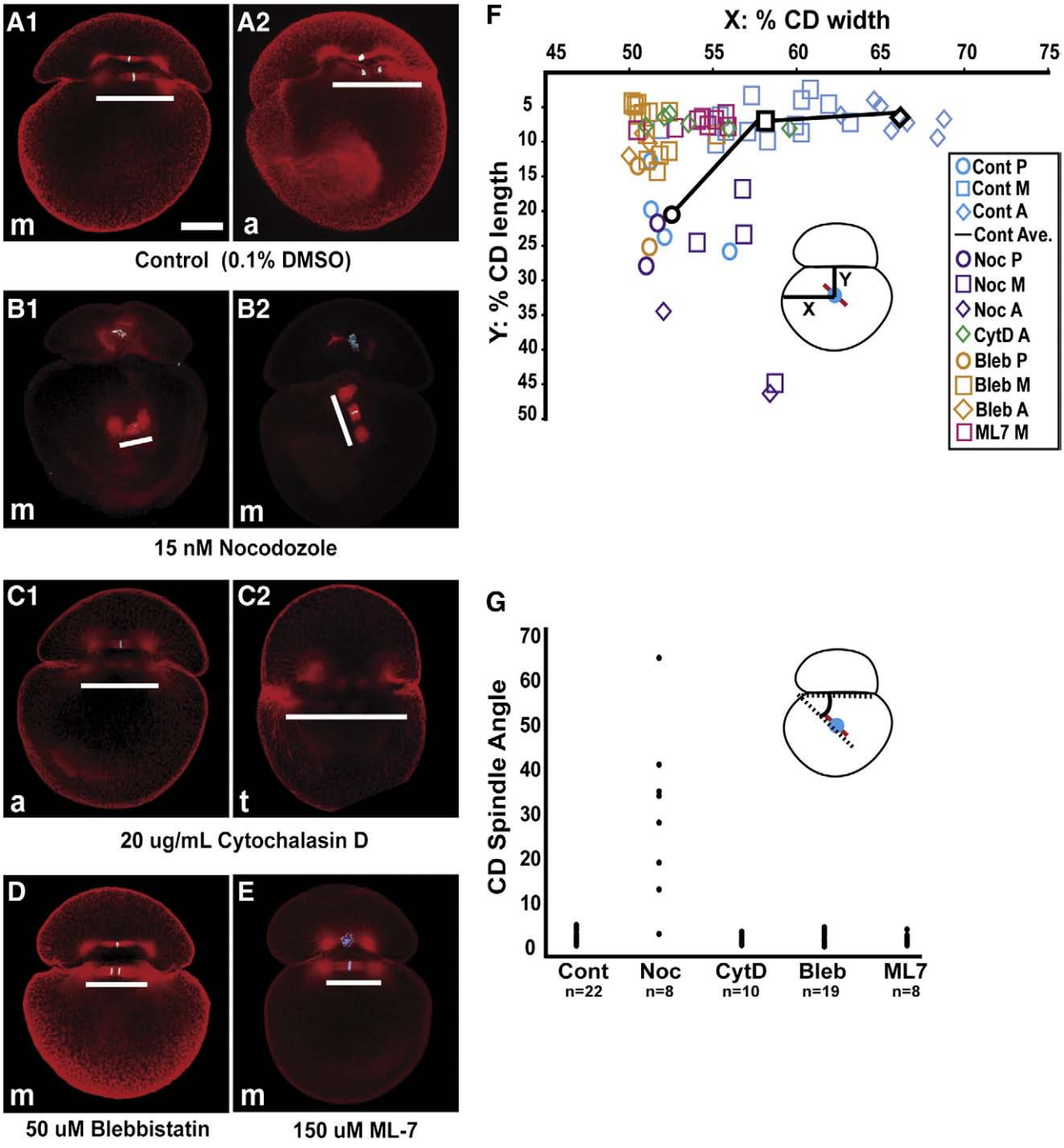

Fig. 4. Drug-specific disruption of MA dynamics. (A–E) Confocal images of control and drug-treated embryos, stained for tubulin (red) and histone (blue), when sibling controls were at metaphase (m), anaphase (a) or telophase (t); white bars parallel each spindle. (A1–2) Control embryos cultured in media with DMSO at a concentration equivalent to that used in the drug treatments. (B–E) Examples of embryos treated with drugs continuously from 265′ AZD until fixation, 110–140 min later. (B1–2) in embryos treated with low levels of nocodazole, one or both asters fail to attach to the AB/CD interface, so that the position and angle of the spindle are highly variable; cortical staining is also reduced. (C1–2) In embryos treated with cytochalasin D, both spindle poles remain in contact with the interface, but the MA does not move towards the right side of the embryo, and the spindle are longer than in controls (C2). (D and E) In embryos treated with either blebbistatin or ML-7, the spindle poles remain in contact with the interface and the spindle length is normal, but the MA does not move rightward. (F) Graphical representation of spindle midpoint position (inset) in controls and drug treatments at various time points in mitosis. P (prophase), M (metaphase), A (anaphase); The black line shows the progression of the average position of the spindle midbody for the control embryos. (G) Distribution of CD spindle-interface angles (inset) measured in a total of 67 control and drug-treated embryos. Scale bar, 100 μm.

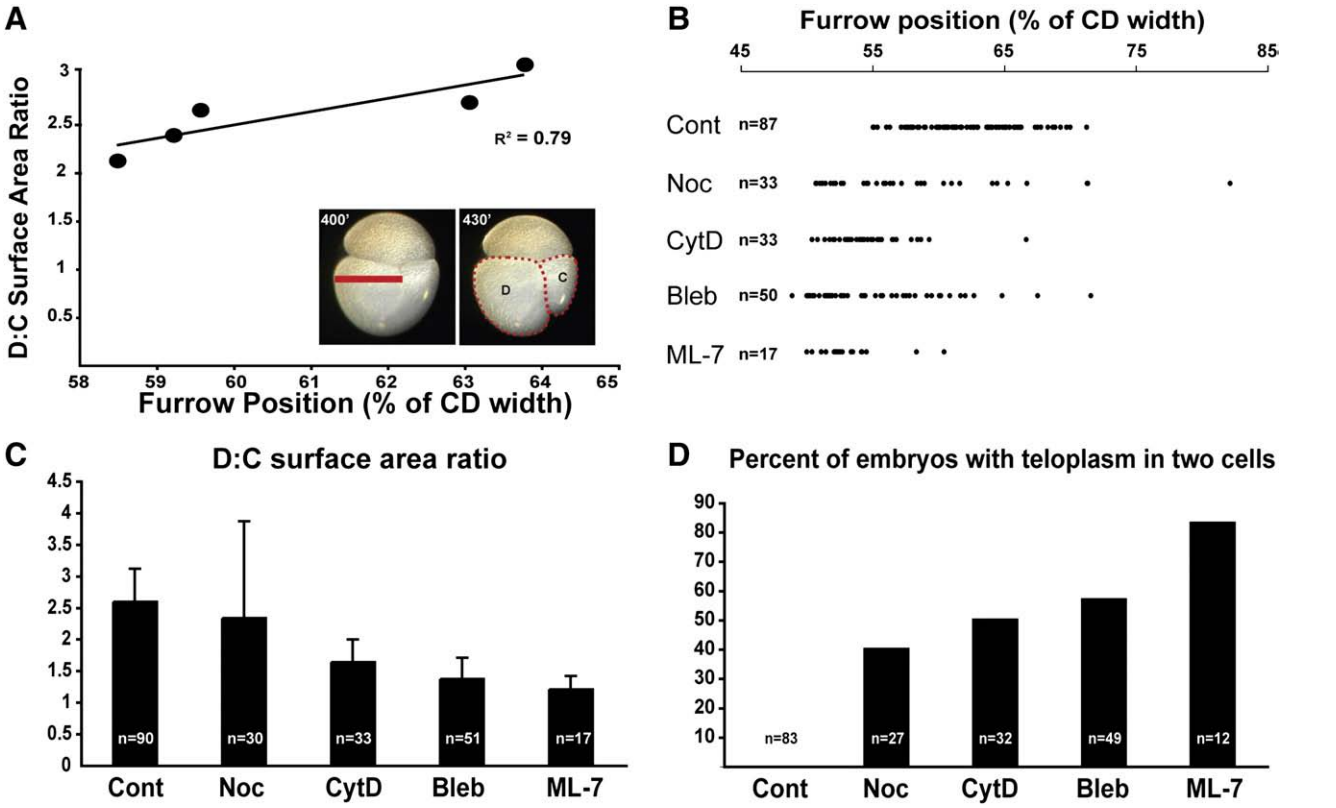

Fig. 5. Perturbation of CD cleavage by drug treatments. Control and drug treatments are described in Fig. 4. (A) Measurements taken from time lapse movies of individual embryos show a strong correlation between the position of the early cleavage furrow relative to the maximum CD width at the onset of cytokinesis (~400′ AZD, red bar in inset) and the D:C surface area ratio near the end of cytokinesis (~430′ AZD, red dotted outline inset). For (B) and (C), either furrow position or D:C surface area ratio was measured in batches of treated embryo D; in (C), the large standard error in nocodazole-treated embryos reflects an apparent randomization of CD cleavage resulting from disruption of the association of the MA and the anterior cortex (see Fig. 4). (D) Percentage of control and drug-treated embryos in which teloplasm was present in both cells following CD division.

embryos treated with drugs that interfere with the microtubule and actomyosin cytoskeletons.

To establish a baseline for analysis of CD divisions in drug-treated embryos, we first quantified the degree of cleavage inequality of the CD cell in control embryos (Fig. 5A). For this purpose we measured the placement of the cytokinetic furrow relative to CD cell width at the start of second cleavage (~400′ AZD), and for the same embryos, the ratio of the area enclosed by the D cell and C cell outlines near the end of CD cleavage (~420′ AZD; Fig. 5A). For these 5 embryos from a single batch, we found that there is a high correlation between the placement of the furrow and the ratio of the cell surfaces (Fig. 5A). Due to technical considerations, the following data obtained during inhibitor studies were taken from embryos at a broader range of time points. Nonetheless, the range and average values obtained for these measurements allowed us to distinguish drug-treated from control embryos in the experiments described below (Figs. 5B–D).

Apposition of the MA to the basolateral cortex is microtubule-dependent

Embryos were raised in control (DMSO) or nocodazole solutions (15 nM nocodazole) from the beginning of the 2-cell stage (~265′ AZD; Figs. 4–6); treating embryos with 20 nM nocodazole beginning of the 2-cell stage prevented cytokinesis (data not shown).

Cortical and astral microtubules were greatly reduced in nocodazole-treated embryos relative to controls, but central spindles were still visible (Fig. 4B); in every case ($n=8$) one or both spindle poles lay further from the anterior cortex of the CD cell compared to controls ($n=27$; Fig. 4F). As a result, the spindles in nocodazole-treated embryos were often misaligned with respect to the AB/CD interface; the angle between the interface and the spindle ranged from 4° to 66° ($n=8$), whereas that in control embryos ranged from 1° to 6° ($n=24$; Fig. 4G). Even in those experimental embryos in which the spindle remained parallel to the interface, neither spindle pole made close contact with the interface, so the entire MA was positioned more centrally within the cytoplasm (Fig. 4B).

Consistent with the wide range of spindle orientations observed in nocodazole-treated embryos at early time points (Fig. 4), a broad range of cleavage plane orientations and positions were observed when nocodazole-treated embryos were raised to later time points (Figs. 5B–C, 6D–F). The position of the furrow in nocodazole-treated embryos ranged from 50% to 80% of the width of the embryo as defined above, with a median of 56% ($n=33$), a broader range than in controls (Figs. 5B, 6B, E). Likewise, the projected surface area ratios measured for the C and D cells in nocodazole-treated embryos were variable compared with controls (Fig. 5C). The D:C ratio of projected surface areas in nocodazole-treated embryos ranged from 1 to 7 with a median ratio of 1.9 ($n=30$). These values reflect the fact that in nocodazole-treated embryos, CD divisions were either more equal or more unequal than compared to controls (Fig. 6F). It is important to note that in some of the abnormally unequal divisions, the smaller cell was born at the animal pole (data not shown), underscoring the fact that reducing microtubules can randomize the orientation of CD division. Finally, while teloplasm was segregated exclusively to the D cell at second cleavage in all control embryos ($n=83$), teloplasm was distributed among both of the CD daughter cells in 40% (12 of 27) of nocodazole-treated embryos (Figs. 5D, 6F). Together, these data suggest that the close association between the spindle poles and the anterior cortex of the CD cell is dependent on astral microtubules.

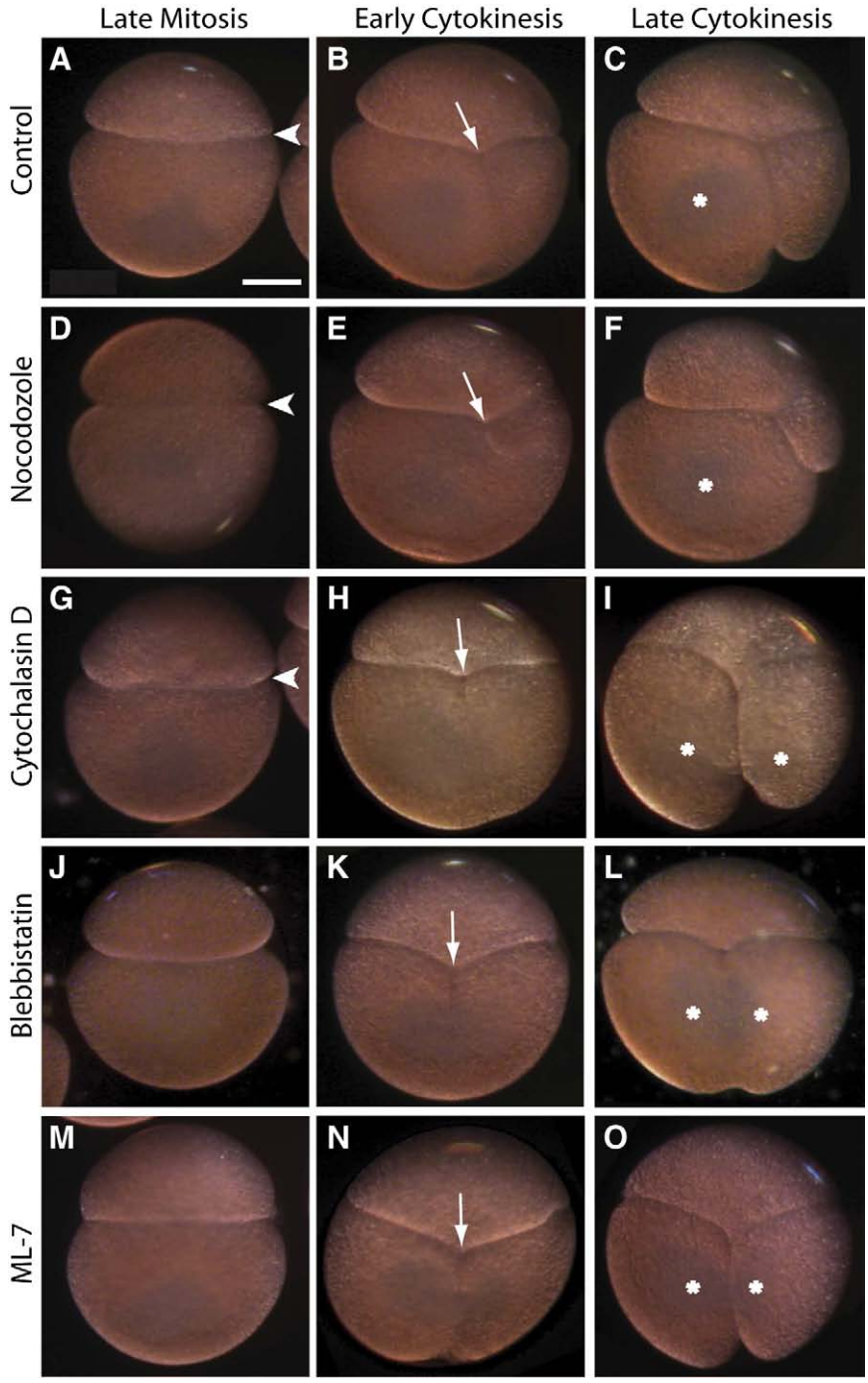

Fig. 6. Actomyosin inhibitors block asymmetrization of the AB/CD interface. Representative images of live control and drug-treated embryos treated as in Figs. 4, 5. (A–C) Control embryos invariably develop an asymmetric apposition of AB and CD on the right side (A, arrowhead), the cytokinetic furrow is displaced to the right (B, arrow) and only the D cell inherits teloplasm (C, asterisk). (D–F) In embryos treated with 15 nM nocodazole from the beginning of the 2-cell stage, the asymmetric apposition of the AB and CD cells is apparently normal but the position and orientation of the cleavage furrow are highly variable; in this example, the CD cleavage is more highly unequal than in controls. (G–I) In embryos treated with 10 μg/mL cytochalasin D, the asymmetric apposition of the blastomeres may be reduced but is still evident (G). As illustrated here, many such embryos divide more equally than controls (H) and both daughter cells inherit teloplasm (I). (J–O) In most embryos treated with either 50 μM blebbistatin or 150 μM ML-7, the asymmetric apposition of AB and CD does not develop (J, M); cleavage furrow is centrally located (K, N); and both daughter cells inherit teloplasm (L, O). Scale bar, 100 μm.

Involvement of the actomyosin cytoskeleton in the unequal CD cleavage

The association of the MA with cortical domains at the AB/CD interface during metaphase of the CD cell cycle (Fig. 3) suggested a critical interaction between the MA and cortical factors such as the actin cytoskeleton. If so, the displacement of the MA could be under the control of an actomyosin network. To test this possibility, we first treated embryos with cytochalasin D (cytD; Figs. 4C, 5, 6G–I). Cytokinesis failed to complete at cytD concentrations of 20 μM and above, so embryos intended for analysis of cleavage inequality were treated with 10 μM cytD. Otherwise, 20 μM cytD was used and failure to complete cytokinesis was taken to indicate the efficacy of the drug.

In contrast to the results obtained with nocodazole, cytD treatment did not prevent the close apposition of the MA spindle poles and the cortex of the AB/CD interface in the CD cell (Figs. 4C, F). In all embryos

examined ($n = 10$), both spindle poles contacted the interface, and the spindle remained close to the anterior cortex of the CD cell. The spindle was frequently longer in cytD-treated embryos than in controls by anaphase (Fig. 4C), and the movement of the spindle towards the right side of the embryo was less pronounced in cytD-treated embryos relative to controls (Fig. 4F). The angle between the CD spindle and the interface was similar to that in control embryos (Fig. 4G). The second cleavage furrow in cytD-treated embryos formed closer to the center of the cell than in controls, with a median placement of 54% of the CD width ($n = 33$ Figs. 5B, 6H). Embryos exposed to cytD showed more equalized CD cleavage (Figs. 5C, 6I) and the median projected surface area ratios for these embryos were significantly smaller (1.5, $n = 34$) than for controls (2.5, $n = 60$, Student's t-test $p \leq 0.0001$; Fig. 5C). In many embryos (50%, 16 of 32), both daughter cells of the CD cleavage inherited teloplasm (Figs. 5D, 6I). These results suggested that inhibiting the formation of microfilaments did not prevent the association between the CD spindle poles and the interface cortex (Figs. 4C, F, G), but did result in a more equal division of the CD cell (Figs. 5B–D, 6I), by reducing the rightward movement of the MA (Fig. 4F).

To test for possible L–R asymmetries in the actomyosin cytoskeleton, two immunohistochemical approaches were tried. Staining embryos for a polyclonal antibody that recognizes actin revealed no left–right asymmetry (Fig. S1B). In contrast, staining embryos with an antibody raised against a phosphorylated epitope of mammalian myosin regulatory light chain (p-rMLC) often gave asymmetric staining patterns (Fig. S1A). However, the observed asymmetry bore no consistent relationship to the L–R – or any other – embryonic axis, nor was this staining affected by treatment with ML-7, a small inhibitor of myosin light chain kinase that should block one pathway to activation of the myosin light chain (Saitoh et al., 1987) and which dramatically equalize CD cleavage (see following paragraph). Thus, this result was not pursued further.

To ask if actomyosin contractility played a role in setting up the unequal CD cleavage, embryos were treated with either 50 μM blebbistatin [which inhibits non-muscle myosin II; Straight et al., 2003], or 150 μM ML-7 (Saitoh et al., 1987). Strikingly, both treatments equalized the CD cleavage more completely than either cytD or nocodazole treatment (Figs. 5, 6). As with cytD treatment, neither blebbistatin nor ML-7 treatment prevented the association of the CD spindle poles with the anterior cortex (Figs. 4D–F), but the CD spindle failed to shift towards the right side of the cell in these embryos ($n = 19$, 8 respectively; Figs. 4D–F). Also the angle of the spindle was similar to those found in control embryos (Fig. 4G). The placement of the second cleavage furrow in these treatments was near the middle of the cell (Figs. 5B, 6K, N), with a median position at 52% of CD width for both blebbistatin ($n = 50$) and ML-7 ($n = 17$). The median projected D:C surface area ratio was 1 for ML-7 ($n = 16$) and 1.26 for blebbistatin ($n = 53$; Fig. 5C). In both treatments teloplasm was frequently inherited by both daughter cells (57% for blebbistatin, $n = 49$ and 83% for ML-7, $n = 12$; Figs. 5D, 6L, O).

Finally, blebbistatin- and ML-7-treated embryos also failed to develop the more pronounced apposition of AB and CD blastomeres on the right side of the embryo, and thus remained bilaterally symmetric relative to control embryos (Figs. 6J, M). In contrast in cytD and nocodazole-treated embryos the L–R asymmetry was still observed, though to a lesser extent in cytD (Figs. 6D, G).

Discussion

The unequal cleavage of the CD cell is critical for establishing the second embryonic axis in *Helobdella* and other unequally cleaving spiralians. In the work presented here, we show that the unequal cleavage is controlled by the rightward displacement of a symmetric MA in an actomyosin-dependent process (Fig. 7).

Centrosome duplication in the nascent CD cell is already complete as the zygote is undergoing cytokinesis. The spindle moves toward the AB/CD interface, capturing the nucleus en route. At prophase, the CD MA forms in apposition to the vegetal portion of the blastocoel wall (Figs. 1, 3). As the blastocoel shrinks, the asters remain attached to the cortex which becomes part of the AB–CD interface on the left and right sides of the blastocoel, respectively (Figs. 1, 3). This attachment is microtubule-dependent (Fig. 4), and critical for normal CD division, as revealed by its nocodazole sensitivity (Figs. 5, 6).

Bilateral symmetry of the embryo, including the position of the CD MA is maintained until metaphase, when the MA and the blastocoel

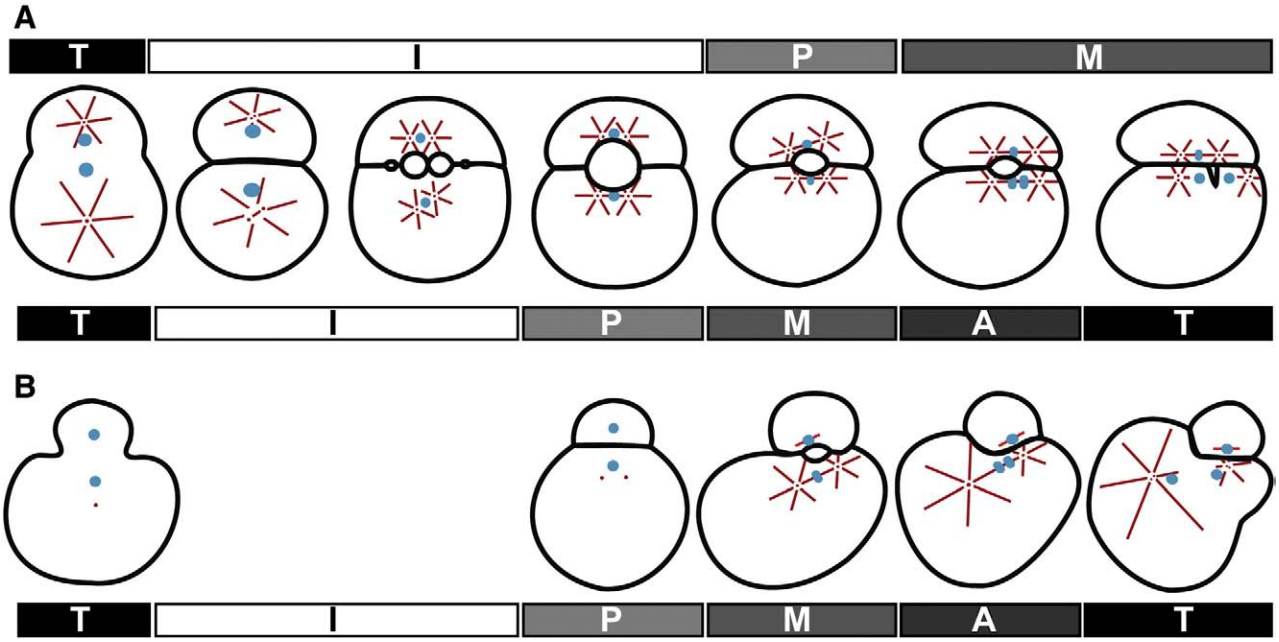

Fig. 7. Divergent processes effect the division of a homologous, unequal cleavage in *Helobdella* and *Tubifex*. (A) Events leading up to the unequal CD division in *Helobdella*; animal pole views with AB at top, CD at bottom. Bars above the embryos show the AB cell cycle, while those below the embryos show the CD cell cycle. Microtubules are depicted as red lines, centrosomes as red dots, and chromatin in blue. (B) Events leading up to the unequal CD division in *Tubifex*; animal pole views with AB at top, CD at bottom. See text for details.

become displaced toward the right (prospective C) side of the embryo (Fig. 3). This movement coincides with the first external L–R asymmetry, as the AB and CD cells become more closely apposed on their right sides (Fig. 2).

The rightward displacement of the symmetric MA is a microfilament-dependent process (Fig. 4), apparently driven by actomyosin contractility. Treating embryos with cytochalasin D, blebbistatin or ML-7 at the 2-cell stage tended to equalize CD cleavage, without blocking the attachment of the MA to the interface (Figs. 4–6). The asymmetric apposition of the blastomeres is also blocked by blebbistatin and ML-7 (Fig. 6), but not by nocodazole (Fig. 6), suggesting that the actomyosin contraction is independent of the spindle-cortex apposition.

Unequal first and second cleavages in Helobdella are controlled by different mechanisms

In *Helobdella* the unequal first cleavage entails an initially symmetric MA that becomes asymmetric during metaphase, following the transient down-regulation of one centrosome and the partial collapse of the associated aster (Ren and Weisblat, 2006). Previous work suggests that the first unequal cleavage relies on cortex-independent mechanisms (Nelson and Weisblat, 1992; Ren and Weisblat, 2006).

In contrast, during the 2-cell stage, the existence of the AB/CD interface is a possible source of polarity cues not present in the zygote, and our results demonstrate that the second unequal cleavage requires a close interaction between the MA and the AB/CD interface (Figs. 4–6). Moreover, the centrosomes and MA remain symmetric throughout mitosis (Fig. 3), and CD cleavage is equalized by inhibitors of actomyosin contractility (Figs. 4–6) that do not affect first cleavage (data not shown). Thus, the inequalities of the first and second cleavages in *Helobdella* are established by dramatically distinct processes.

Previous work showed that when CD and AB cells are separated at first cleavage, the isolated CD cells frequently divide equally (Symes and Wiesblat, 1992). Deforming an isolated CD cell with a glass bead (within the confines of an agarose well) partially rescued the inequality of the CD cleavage, but the effect on MA position was not examined in those experiments. Since then, a direct effect of mechanical deformation on MA positioning has been demonstrated for the *C. elegans* P_1 cell (Tsou et al., 2003). These authors proposed that lateral attachment of microtubules to a flattened cell cortex results in a larger pulling force for those microtubules intersecting the cortex at a shallow angle.

The fact that mechanical deformation of the CD cell by the AB cell contributes to establishing the unequal CD cleavage in *Helobdella* does not rule out a possible role for inductive interactions acting in parallel. Circumstantial evidence in favor of the latter possibility comes from observations that Wnt, Notch, and MAPK signaling components are expressed in a dynamic, mutually exclusive pattern in AB and CD during interphase of the 2-cell stage (Gonsalves and Weisblat, 2007; Huang et al., 2001); the exclusivity of the Wnt expression involves inhibitory interactions between cells AB and CD (Huang et al., 2001). Whether this intercellular signaling at the 2-cell stage is critical for the unequal CD cleavage remains to be determined.

Given that the AB MA also associates with the AB/CD interface and then moves rightward during metaphase as it “tracks” the CD MA (Fig. 3), why doesn't the AB cell divide unequally like CD? The key to resolving this paradox appears to be the differences in AB and CD cell cycle duration. Although the mechanisms are not yet known, the cell cycles of D quadrant cells and their precursors are accelerated relative to blastomeres that do not inherit teloplasm. Thus, the AB MA shifts rightward with the CD MA (Fig. 3, compare the AB MA in 390′ and 395′), but then as CD initiates cytokinesis, the rightward directed “traction” forces seem to turn off, and the AB MA shifts back towards the center before that cell initiates cytokinesis (Fig. 3, compare the AB MA in 395′ and 405′).

The establishment of L–R chirality in Helobdella

Few, if any, bilaterian species are truly bilaterally symmetric even at the intermediate level of cells and tissues, and therefore the establishment of asymmetries along the left–right axis is of general interest in development. Within the spiralians it is of particular interest since in groups such as the gastropods the chirality of early cleavages correlates with overt larval and adult asymmetries such as shell coiling (Freeman and Lundelius, 1982), and later in development gastropods use similar molecular mechanisms as deuterostomes to pattern the left–right axis (Grande and Patel, 2009). In equally cleaving spiralians, the dextral or sinistral rotation of micromeres relative to macromeres at third cleavage is the canonical early marker of handedness (Shibazaki et al., 2004). In unequally cleaving spiralians, bilateral symmetry is broken at second cleavage by the unequal CD division.

It should be noted that these two symmetry breaking processes are not necessarily fixed or linked within or among species (Dorresteijn, 2005; Luetjens, 1995). A dramatic example is the zebra mussel, *Dreissena* (Luetjens, 1995; Luetjens and Dorresteijn, 1998b), in which the chirality of the CD cleavage and of micromere formation vary independently, resulting in four distinct 8-cell stage morphs, all of which develop normally.

Work presented here suggests that the establishment of L–R asymmetry in *Helobdella* at second cleavage is under the control of the actomyosin network. Our results do not speak directly to the question of how the chirality of the L–R asymmetry is initially established, but in other unequal cleavers, the chirality of the second cleavage correlates with sperm entry point (SEP), with the SEP being closer to the C cell (Luetjens and Dorresteijn, 1998b; Morgan and Tyler, 1930, 1938; van den Biggelaar and Guerrier, 1983). The idea that signaling cascades initiated by sperm entry bias actomyosin contractility is consistent with a large body of work in many species demonstrating that SEP determines one of the body axes (Elinson, 1975; Goldstein and Hird, 1996; Sardet et al., 2007), and that the SEP signal is transduced by actomyosin contractility (Sardet et al., 2007; Severson and Bowerman, 2003). In *Helobdella*, fertilization is internal, and it has not yet been possible to visualize the SEP in the large yolky egg so as to correlate it with subsequent cleavage patterns. It will be interesting to test whether the actomyosin skeleton is involved in the chirality of the early spiral cleavage pattern in other spiralians, especially those in which SEP can be correlated with cleavage patterns.

Divergent mechanisms underlie unequal second cleavage in the clitellate annelids Helobdella and Tubifex

Abundant evidence supports the hypothesis that oligochaetes and leeches form a monophyletic group, for which D quadrant specification by unequal cleavage is an ancestral trait (Dohle, 1999). The work presented here adds to previous studies showing that the cell biological mechanisms of D quadrant specification have diverged extensively in the *H. robusta* species complex as compared with the sludge worm *Tubifex*, an oligochaete (Ishii and Shimizu, 1995, 1997; Ren and Weisblat, 2006; Shimizu, 1982b, 1996b; Shimizu et al., 1998).

Regarding the second cleavage, Takahashi and Shimizu (Takahashi and Shimizu, 1997) have shown that the CD MA in *Tubifex* becomes asymmetric prior to cleavage, unlike in *Helobdella* (Fig. 7). In this case, when the CD MA first forms it is biastral and symmetrical, and both spindle poles are near with anterior cortex. By anaphase the spindle pole on the prospective C side remains small and in close contact with the cortex, while the prospective D spindle pole is large and distant from the interface (Fig. 7). Moreover, when the connection between the C spindle pole and the cortex was disrupted by centrifugation or

cytochalasin D treatment, the CD cell divided equally (Takahashi and Shimizu, 1997).

We note two differences between *Helobdella* and *Tubifex* that might contribute to the differences in the CD division mechanisms. One difference is that the first cleavage is more unequal in *Tubifex* than in *Helobdella* (Fig. 7). As a result, the AB/CD interface is much smaller in *Tubifex*, and there simply may not be room for both poles of the CD MA to attach to the interface, especially as the MA lengthens in late metaphase and anaphase (Fig. 7).

A second difference between the two species is that in *Tubifex* the AB cell does not inherit a centrosome at first cleavage (Shimizu, 1996a). The anastral AB MA in *Tubifex* resides near the interface as a single focal point of dense microtubules throughout the cell cycle, and the right (prospective C) pole of the CD MA attaches to the interface opposite that point (Shimizu et al., 1998). In *Helobdella*, the AB MA also attaches to the interface, but in contrast to *Tubifex*, this biastral MA attaches at two distinct sites at the interface and each spindle pole of the CD MA attaches to one of them, thereby maintaining symmetry of the CD MA.

Conclusions

Comparisons of *Tubifex* and *Helobdella* development illustrate the extent to which cell biological mechanisms underlying a highly conserved process (in this case, D quadrant specification in clitellate annelids) can diverge significantly during evolution, and provide clues regarding the constraints and permissions under which this divergence occurred. Given that such cryptic variation in basic cell biological processes may accumulate within evolutionary lineages, it seems likely that this can also set the stage for situations where further minor changes in one lineage relative to the other lead to an abrupt, macroscopic change in the spiral cleavage program itself. It seems likely that this model applies to the evolutionary transformation of other developmental processes as well.

Acknowledgments

We thank the Cande and Welch labs for the generous gifts of the urchin tubulin antibody and blebbistatin, respectively, and the Levine lab for the generous use of their confocal microscope. We also thank Dr. Jen Yi Lee for helpful discussions, advice and for sharing reagents. We thank Crystal Chaw, Dr. Dian-Han Kuo, Stephanie Gline and Dr. Yvonne Valles for their comments on the manuscript. This work was supported by NSF grant 0314718 and NIH grant R01 GM074619 to D. AW.

Appendix A. Supplementary data

Supplementary data associated with this article can be found, in the online version, at doi:10.1016/j.ydbio.2009.07.007.

References

Arnolds, W.J.A., van den Biggelaar, J.A.M., Verdonk, N.H., 1983. Spatial aspects of cell interactions involved in the determination of dorsoventral polarity in equally cleaving gastropods and regulative abilities of their embryos, as studied by micromere deletions in *Lymnaea* and *Patella*. Roux's Arch. Dev. Biol. 192, 75–85.

Astrow, S., Holton, B., Weisblat, D.A., 1987. Centrifugation redistributes factors determining cleavage patterns in leech embryos. Dev. Biol. 120, 270–283.

Astrow, S.H., Holton, B., Weisblat, D.A., 1989. Teloplasm formation in a leech, *Helobdella triserialis*, is a microtubule-dependent process. Dev. Biol. 135, 306–319.

Bely, A.E., Weisblat, D.A., 2006. Lessons from leeches: a call for DNA barcoding in the lab. Evol. Dev. 8, 491–501.

Bissen, S.T., Weisblat, D.A., 1989. The durations and compositions of cell cycles in embryos of the leech, *Helobdella triserialis*. Development 106, 105–118.

Blair, S.S., Weisblat, D.A., 1984. Cell interactions in the developing epidermis of the leech *Helobdella triserialis*. Dev. Biol. 101, 318–325.

Clement, A.C., 1952. Experimental studies on germinal localization in *Ilyanassa*. I. the role of the polar lobe in determination of the cleavage pattern and its influence in later development. J. Exp. Zool. 121, 593–626.

Cowan, C.R., Hyman, A.A., 2004. Asymmetric cell division in *C. elegans*: cortical polarity and spindle positioning. Annu. Rev. Cell Dev. Biol. 20, 427–453.

Dohle, W., 1999. The ancestral cleavage pattern of the clitellates and its phylogenetic deviations. Hydrobiologia 402, 267–283.

Dorresteijn, A., 2005. Cell lineage and gene expression in the development of polychaetes. Hydrobiologia 535–536, 1–22.

Dorresteijn, A.W.C., Bornewasser, H., Fischer, A., 1987. A correlative study of experimentally changed first cleavage and Janus development in the trunk of *Platynereis dumerilii* (Annelida, Polychaeta). Roux's Arch. Dev. Biol. 196, 51–58.

Dunn, C.W., Hejnol, A., Matus, D.Q., Pang, K., Browne, W.E., Smith, S.A., Seaver, E., Rouse, G.W., Obst, M., Edgecombe, G.D., Sørensen, M.V., Haddock, S.H., Schmidt-Rhaesa, A., Okusu, A., Kristensen, R.M., Wheeler, W.C., Martindale, M.Q., Giribet, G., 2008. Broad phylogenomic sampling improves resolution of the animal tree of life. Nature 452, 745–749.

Elinson, R.P., 1975. Site of sperm entry and a cortical contraction associated with egg activation in the frog *Rana pipiens*. Dev. Biol. 47, 257–268.

Erseus, C., Kallersjo, M., 2004. 18S rDNA phylogeny of Clitellata (Annelida). Zool. Scr. 33, 187–196.

Fernández, J., Olea, N., 1982. Embryonic development of glossiphoniid leeches. In: Harrison, F.W., Cowden, R.R. (Eds.), Developmental Biology of Freshwater Invertebrates. Alan R. Liss, New York, NY, pp. 317–361.

Fernández, J., Olea, N., Téllez, V., Matte, C., 1990. Structure and development of the egg of the glossiphoniid leech *Theromyzon rude*: reorganization of the fertilized egg during completion of the first meiotic division. Dev. Biol. 137, 142–154.

Freeman, G., Lundelius, J.W., 1982. The developmental genetics of dextrality and sinistrality in the gastropod *Lymnaea peregra*. Roux's Arch. Dev. Biol. 191, 69–83.

Freeman, G., Lundelius, J.W., 1992. Evolutionary implications of the mode of D quadrant specification in coelomates with spiral cleavage. J. Evol. Biol. 5, 205–247.

Giribet, G., 2008. Assembling the lophotrochozoan (=spiralian) tree of life. Philosophical Transactions of the Royal Society of London series B. 363, 1513–1522.

Glotzer, M., 2004. Cleavage furrow positioning. J. Cell Biol. 164, 347–351.

Goldstein, B., Hird, S.N., 1996. Specification of the anteroposterior axis in *Caenorhabditis elegans*. Development 122, 1467–1474.

Gonsalves, F.C., Weisblat, D.A., 2007. MAPK regulation of maternal and zygotic Notch transcript stability in early development. Proc. Natl. Acad. Sci. U. S. A. 104, 531–536.

Goulding, M., 2003. Cell contact-dependent positioning of the D cleavage plane restricts eye development in the *Ilyanassa* embryo. Development 130, 1181–1191.

Grande, C., Patel, N.H., 2009. Nodal signalling is involved in left–right asymmetry in snails. Nature 457, 1007–1011.

Halanych, K.M., Bacheller, J.D., Aguinaldo, A.M.A., Liva, S.M., Hillis, D.M., Lake, J.A., 1995. Evidence from 18S ribosomal DNA that the lophophorates are protostome animals. Science 267, 1641–1643.

Hejnol, A., Pfannenstiel, H.-D., 1998. Myosin and actin are necessary for polar lobe formation and resorption in *Ilyanassa obsoleta* embryos. Dev. Genes Evol. 208, 229–233.

Henry, J.J., 1986. The role of unequal cleavage and the polar lobe in the segregation of developmental potential during first cleavage in the embryo of *Chætopterus variopedatus*. Roux's Arch. Dev. Biol. 195, 103–116.

Henry, J., Martindale, M., 1999. Conservation and innovation in spiralian development. Hydrobiologia 402, 255–265.

Henry, J.Q., Perry, K.J., Martindale, M.Q., 2006. Cell specification and the role of the polar lobe in the gastropod mollusc *Crepidula fornicata*. Dev. Biol. 297, 295–307.

Huang, F.Z., Bely, A.E., Weisblat, D.A., 2001. Stochastic WNT signaling between non-equivalent cells regulates adhesion but not fate in the two-cell leech embryo. Curr. Biol. 11, 1–7.

Inoue, S., Dan, K., 1987. Studies of unequal cleavage in mollusks. 2. Asymmetric nature of the 2 asters. Int. J. Invertebr. Reprod. Dev. 11, 335–353.

Ishii, R., Shimizu, T., 1995. Unequal first cleavage in the *Tubifex* egg: involvement of a monastral mitotic apparatus. Development, Growth and Differentiation 37, 687–701.

Ishii, R., Shimizu, T., 1997. Equalization of unequal first cleavage in the *Tubifex* egg by introduction of an additional centrosome: implications for the absence of cortical mechanisms for mitotic spindle asymmetry. Dev. Biol. 189, 49–56.

Jackson, J.B.C., Kirby, M.X., Berger, W.H., Bjorndal, K.A., Botsford, L.W., Bourque, B.J., Bradbury, R.H., Cooke, R., Erlandson, J., Estes, J.A., Hughes, T.P., Kidwell, S., Lange, C.B., Lenihan, H.S., Pamdolfi, J.M., Peterson, C.H., Steneck, R.S., Tegner, M.J., Warner, R.R., 2001. Historical overfishing and the recent collapse of coastal ecosystems. Science 293, 629–639.

Lambert, J.D., 2008. Mesoderm in spiralians: the organizer and the 4d cell. J. Exp. Zool. 310B, 15–23.

Lambert, J.D., Nagy, L.M., 2001. MAPK signaling by the D quadrant embryonic organizer of the mollusc *Ilyanassa obsoleta*. Development 128, 45–56.

Luetjens, C.M., 1995. Multiple, alternative cleavage patterns precede uniform larval morphology during normal development of *Dreissena polymorpha* (Mollusca, Lamellibranchia). Roux's Arch. Dev. Biol. 205, 138–149.

Luetjens, C.M., Dorresteijn, A.W.C., 1998a. Dynamic changes of the microtubule system corresponding to the unequal and spiral cleavage modes in the embryo of the zebra mussel, *Dreissena polymorpha*. Zygote 6, 239–248.

Luetjens, C.M., Dorresteijn, A.W.C., 1998b. The site of fertilisation determines dorsoventral polarity but not chirality in the zebra mussel embryo. Zygote 6, 125–135.

Martindale, M.Q., Doe, C.Q., Morrill, J.B., 1985. The role of animal–vegetal interaction with respect to the determination of dorsoventral polarity in the equal-cleaving spiralian, *Lymnaea palustris*. Roux's Arch. Dev. Biol. 194, 281–295.

Mescheryakov, V., 1976. Asymmetrical cytotomy and spindle orientation in early isolated blastomeres of gastropod mollusks. Ontogenez 7, 471–477.

Morgan, T.H., Tyler, A., 1930. The point of entrance of the spermatozoon in relation to

the orientation of the embryo in eggs with spiral cleavage. Biol. Bull. (Woods Hole, MA). 58, 59–73.
Morgan, T.H., Tyler, A., 1938. The relation between entrance point of the spermatozoön and bilaterality of the egg of *Chætopterus*. Biol. Bull. (Woods Hole, MA). 74, 401–402.
Nelson, B.H., Weisblat, D.A., 1991. Conversion of ectoderm to mesoderm by cytoplasmic extrusion in leech embryos. Science 253, 435–438.
Nelson, B.H., Weisblat, D.A., 1992. Cytoplasmic and cortical determinants interact to specify ectoderm and mesoderm in the leech embryo. Development 115, 103–115.
Rappaport, R., 1996. Cytokinesis in Animal Cell. Cambridge University Press, Cambridge.
Raven, C.P., 1966. Morphogenesis: the Analysis of Molluscan Development. Pergamon, Oxford.
Ren, X., Weisblat, D.A., 2006. Asymmetrization of first cleavage by transient disassembly of one spindle pole aster in the leech *Helobdella robusta*. Dev. Biol. 292, 103–115.
Saitoh, M., Ishikawa, T., Matsushima, S., Naka, M., Hidaka, H., 1987. Selective inhibition of catalytic activity of smooth muscle myosin light chain kinase. J. Biol. Chem. 262, 7796–7801.
Sardet, C., Paix, A., Prodon, F., Dru, P., Chenevert, J., 2007. From oocyte to 16-cell stage: cytoplasmic and cortical reorganizations that pattern the ascidian embryo. Dev. Dyn. 236, 1716–1731.
Schneider, S.Q., Bowerman, B., 2007. b-Catenin asymmetries after all animal/vegetal-oriented cell divisions in *Platynereis dumerilii* embryos mediate binary cell-fate specification. Dev. Cell 13, 73–86.
Severson, A.F., Bowerman, B., 2003. Myosin and the PAR proteins polarize microfilament-dependent forces that shape and position mitotic spindles in *Caenorhabditis elegans*. J. Cell Biol. 161, 21–26.
Shankland, M., Savage, R.M., 1997. Annelids, the segmented worms. In: Gilbert, S.F., Raunio, A.M. (Eds.), Embryology: Constructing the Organism. Sinauer, Sunderland, MA, pp. 219–235.
Shibazaki, Y., Shimizu, M., Kuroda, R., 2004. Body handedness is directed by genetically determined cytoskeletal dynamics in the early embryo. Curr. Biol. 14, 1462–1467.
Shimizu, T., 1982a. Development in the freshwater oligochaete *Tubifex*. In: Harrison, F.W., Cowden, R.R. (Eds.), Developmental Biology of Freshwater Invertebrates. Alan R. Liss, New York, NY, pp. 283–316.
Shimizu, T., 1982b. Ooplasmic segregation in the *Tubifex* egg: mode of pole plasm accumulation and possible involvement of microfilaments. Roux's Arch. Dev. Biol. 191, 246–256.
Shimizu, T., 1996a. Behaviour of centrosomes in early *Tubifex* embryos: asymmetric segregation and mitotic cycle-dependent duplication. Roux's Arch. Dev. Biol. 205, 290–299.
Shimizu, T., 1996b. The first two cleavages in *Tubifex* involve distinct mechanisms to generate asymmetry in mitotic apparatus. Hydrobiologia 334, 269–276.
Shimizu, T., Nakamoto, A., 2001. Segmentation in annelids: cellular and molecular basis for metameric body plan. Zool. Sci. 18, 285–298.
Shimizu, T., Ishii, R., Takahashi, H., 1998. Unequal cleavage in the early *Tubifex* embryo. Development, Growth and Differentiation 40, 257–266.
Siddall, M.E., Borda, E., 2003. Phylogeny and revision of the leech genus *Helobdella* (Glossiphoniidae) based on mitochondrial gene sequences and morphological data and a special consideration of the *triserialis* complex. Zool. Scr. 32, 23–33.
Siddall, M.E., Burreson, E.M., 1998. Phylogeny of leeches (Hirudinea) based on mitochondrial cytochrome *c* oxidase subunit I. Mol. Phylogenet. Evol. 9, 156–162.
Straight, A.F., Cheung, A., Limouze, J., Chen, I., Westwood, N.J., Sellers, J.R., Mitchison, T.J., 2003. Dissecting temporal and spatial control of cytokinesis with a myosin II inhibitor. Science 299, 1743–1747.
Symes, K., Wiesblat, D.A., 1992. An investigation of specification of unequal cleavages in leech embryos. Dev. Biol. 150, 203–218.
Takahashi, H., Shimizu, T., 1997. Role of intercellular contacts in generating an asymmetric mitotic apparatus in the *Tubifex* embryo. Development, Growth and Differentiation 39, 351–362.
Tsou, M.-F. B., Ku, W., Hayashi, A., Rose, L.S., 2003. PAR-dependent and geometry-dependent mechanisms of spindle positioning. J. Cell Biol. 160, 845–855.
van den Biggelaar, J.A.M., Guerrier, P., 1979. Dorsoventral polarity and mesentoblast determination as concomitant results of cellular interactions in the mollusk *Patella vulgata*. Dev. Biol. 68, 462–471.
van den Biggelaar, J.A.M., Guerrier, P., 1983. Origin of spatial organization. The Mollusca, Vol. 3. Academic Press, San Diego, CA, pp. 179–213.
Verdonk, N.H., van den Biggelaar, J.A.M., 1983. Early development and the formation of the germ layers. The Mollusca, Vol. 3. Academic Press, San Diego, CA, pp. 91–122.
Weisblat, D.A., 2007. Asymmetric cell divisions in the early embryo of the leech *Helobdella robusta*. Prog. Mol. Subcell Biol. 45, 79–95.
Weisblat, D.A., Huang, F.Z., 2001. An overview of glossiphoniid leech development. Can. J. Zool. 79, 218–232.
Weisblat, D.A., Huang, F.Z., Isaksen, D.E., Liu, N.-J. L., Chang, P., 1999. The other side of the embryo: an appreciation of the non-D quadrants in leech embryos. Curr. Top. Dev. Biol. 46, 105–132.
Yazdani, U., Terman, J.R., 2006. The semaphorins. Genome Biol. 7, 211.
Zhang, S.O., Weisblat, D.A., 2005. Applications of mRNA injections for analyzing cell lineage and asymmetric cell divisions during segmentation in the leech *Helobdella robusta*. Development 132, 2103–2113.